doi:10.1017/S1431927621005845
Microsc. Microanal. 27 (Suppl 1), 2021
© Microscopy Society of America 2021

Beam broadening of keV electrons in matter calculated by numerical solution of the electron transport equation

Erich Müller[1], Milena Hugenschmidt[2] and Dagmar Gerthsen[3]

[1]Karlsruhe Institute of Technology (KIT), Laboratory for Electron Microscopy (LEM), Engesserstraße 7, 76131 Karlsruhe, Germany, United States, [2]Karlsruhe Institute of Technology, Laboratory for Electron Microscopy, Karlsruhe, Germany, [3]Laboratorium für Elektronenmikroskopie, Karlsruher Institut für Technologie (KIT), Engesserstr. 7, 76131 Karlsruhe, Germany, United States

Electron microscopy at low primary electron energies $E_0 \leq 30$ keV has experienced increasing interest in the past years. At such low electron energies, the signal-to-noise ratio for material contrast is enhanced and knock-on-damage is reduced compared to higher electron energies. However, at lower energies, the mean free path length decreases. Thus, more scattering events take place and the electron beam broadens by multiple scattering in the material, even for small sample thicknesses. This leads to a progressive worsening of the lateral resolution with increasing penetration depth.

Several analytical approaches to determine electron beam broadening have been published. Frequently applied is the analytical description of Goldstein et al. [1] based on Rutherford scattering of electrons in matter. It gives the width b of the beam after passing a sample of thickness t:

$$b = 0.11 \cdot Z/E_0 \cdot (\rho/A)^{0.5} \cdot t^{1.5}. \quad (1)$$

E_0 is the primary electron energy, while the material density ρ, atomic number Z, and atomic mass A account for the investigated material.

Gauvin et al. [2] published an elaborated theory of electron beam broadening. They distinguish scattering regimes by different Hurst exponents H and describe beam broadening b by the analytical expression:

$$b = (0.1167)^{1-2H} \cdot (39437)^{H} \cdot \sqrt{(R/(1-R))} \cdot Z^{(4H+1)/3} \cdot E_0^{-(2H+1)/2} \cdot (\rho/A)^{H} \cdot t^{1+H}. \quad (2)$$

H is 0.5 for the diffusion regime and reaches $H = 1$ close to the ballistic regime for thin samples while values $H < 0.5$ stand for sub-diffusion scattering. R denotes the percentage of the total beam intensity

https://doi.org/10.1017/S1431927621005845 Published online by Cambridge University Press

that defines the beam radius. Hugenschmidt et al. [3] experimentally verified Eq. (2) by scanning transmission electron microscopy for different materials and electron energies.

In this work, we focus on calculating electron beam broadening by numerically solving the electron transport equation in Lewis' formulation [4], similar to the description of Negreanu et al. [5]. However, we have in addition taken into account energy loss by the continuous-slowing-down approximation. Exact solutions for all scattering regimes (single scattering and multiple scattering) are obtained without approximations such as dominant forward scattering and negligible energy loss. 500 coefficients in the Legendre expansion were calculated by using the *N*-point Gauss-Legendre integration formula for different electron energies. Screened Rutherford differential scattering cross-sections were used. Our program CeTE provides the angular distribution and energy of the scattered electrons after propagating a distinct path length *s*. Following Lewis [4], the mean penetration depth $< z >$ and the lateral displacement $r = \sqrt{(< x^2 >)}$ of the scattered electrons were calculated by the method of moments (MM) from the solution of the transport equation [6]. Figure 1 schematically shows the mean penetration depth $< z >$ and lateral displacement of a 20 keV focused primary electron beam in silicon after traveling different path lengths as indicated in Figure 1. The mean depth $< z >$ in matter is always smaller than the traveled path length *s* and their discrepancy increases with increasing *s* due to the lateral displacement of the scattered electrons. Additionally, the path length s is limited by the total range of the electrons in matter. Beam broadening in matter is considered by the lateral displacement $r = \sqrt{(< x^2 >)}$ at the reached depth $< z >$ to cover all scattering regimes up to diffusion and absorption.

The mean beam radius is plotted in Figure 2 by colored lines for different electron energies as a function of the penetration depth in silicon. The values obtained by the analytical equations of Goldstein and Gauvin are plotted by dashed and dash-dotted lines. For comparison reasons, the prefactor in Eq. (1) and $R = 0.68$ in Eq. (2) were adapted accordingly to consider the width of the beam containing 68 % of the electrons. *H* was set to 0.5 in Eq. (2), corresponding to a scattering regime close to diffusion.

For moderate sample thickness and higher primary electron thicknesses, the beam radius calculated by the moments of the transport equation agrees well with the results of the analytical expressions. As soon as the number of scattering events increases, the lateral displacement increases stronger than predicted by Eq. (1) and (2), as can be seen in Figure 2 for 10 keV electrons (solid yellow curve). Also, the penetration depth and the beam broadening approach an upper limit, which cannot be calculated by the analytical equations.

In this work, we have calculated beam broadening and maximum penetration depth by the moments of the numerical solution of the transport equation. This gives insights into electron scattering at all scattering regimes without limitations to the sample thickness and electron energies.

https://doi.org/10.1017/S1431927621005845 Published online by Cambridge University Press

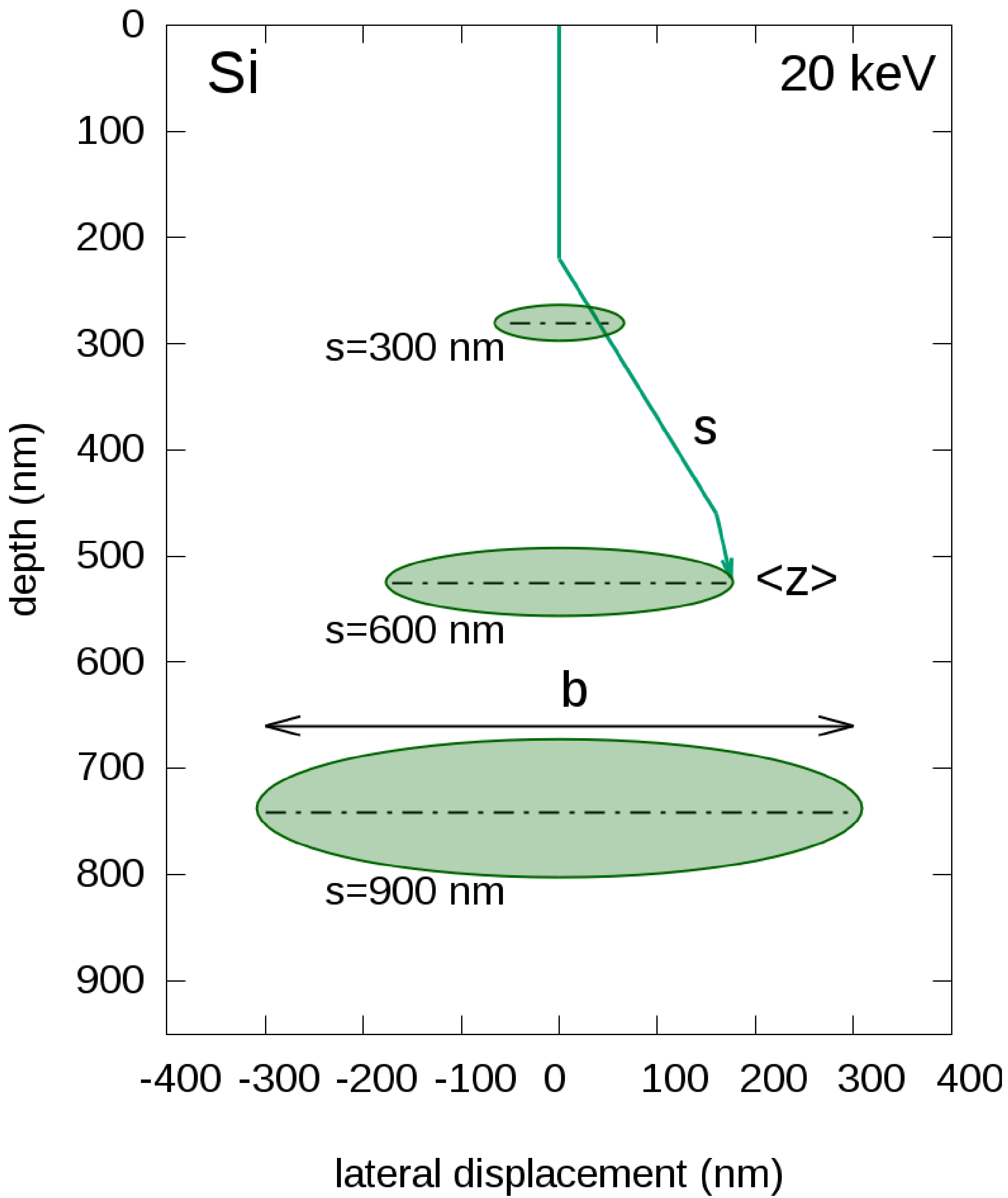

Figure 1. Penetration depth and beam broadening b corresponding to 2r = 2√(<>2>) of 20 keV electrons in silicon for increasing travelled path lengths s.

https://doi.org/10.1017/S1431927621005845 Published online by Cambridge University Press

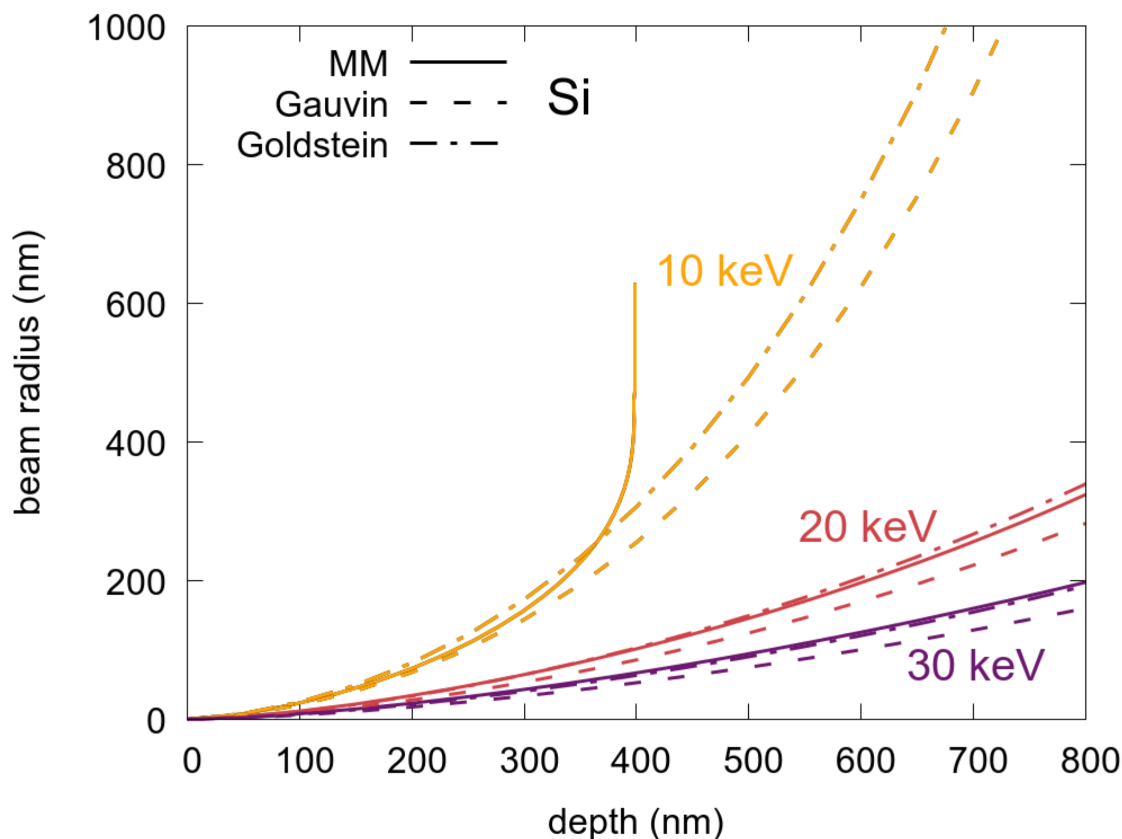

Figure 2. Beam radius as a function of penetration depth for a beam containing 68% of the scattered electrons. Shown are the values for different energies (coloured lines) calculated by the Gauvin (dashed), Goldstein (dashed-dotted), and MM (continuous lines) formalism.

References

[1] J Goldstein et al., Scanning Elecron Microscopy 1 (1977), p. 315.

[2] R Gauvin et al., Ultramicroscopy, 167 (2016), p. 21.

[3] M Hugenschmidt et al., Journal of microscopy 274 (2019), p. 150.

[4] HW Lewis, Phys. Rev. 78 (1950), p. 526

[5] C Negreanu, Radiation Physics and Chemistry 74 (2005), p. 264.

[6] E Müller et al., Phys. Rev. Research 2 (2020), p. 043313

[7] We acknowledge funding by the Deutsche Forschungsgemeinschaft (DFG, German Research Foundation) under Germany's Excellence Strategy – 2082/1 – 390761711.

https://doi.org/10.1017/S1431927621005845 Published online by Cambridge University Press